GeoArabia, Vol. 1, No. 3, 1996
Gulf PetroLink, Bahrain

Application of Neural Networks and Cokriging for Predicting Reservoir Porosity-Thickness (∑øh)

Katsuhei Yoshioka, Nobusuke Shimada
Technology Research Center
Japan National Oil Corporation
and
Yoshiro Ishii
Middle East Representative Office
Japan National Oil Corporation

ABSTRACT

The distribution of the porosity-thickness (∑øh) of the Arab C4 Zone in the offshore El Bunduq field was estimated using neural network and geostatistical techniques. The Arab C4 Zone is approximately 10 to 15 meters thick which corresponds to a time window of less than 20 milliseconds. The reservoir is faulted and the reflection has a poor signal-to-noise ratio. The study utilizes 21 seismic attributes which were derived from a 3-D seismic survey calibrated from 42 wells, 27 of which are deviated. The attributes include different types of amplitudes, complex trace statistics, sequence statistics and frequencies. Three methods are compared: (I) simple kriging using only well data, (II) the neural network technique using 3-D seismic and well data, and (III) cokriging using the output of the neural network technique. Cross validation tests indicate that Method III is not consistently more precise than Method I. Also Method II, in cross-validation tests, demonstrated relatively large dispersion between data and estimates. It appears that although neural networks achieve good correlation between seismic attributes and reservoir properties, the physical relationship remains ambiguous.

INTRODUCTION

El Bunduq field straddles the border between Abu Dhabi and Qatar, in the Arabian Gulf (Figure 1). The field is a domal structure with a width of approximately 7 kilometers (km) superimposed on a northeast-southwest trending anticline (Bashbush et al., 1983). The main producing oil reservoirs are the Jurassic Arab C4 and Arab D zones. The Arab Formation consists mainly of carbonates, accompanied by subordinate anhydrite. The Arab C4 zone is separated from the Arab D by an anhydrite layer 20 feet (ft) thick (Honda et al., 1988).

In El Bunduq the Arab reservoirs are vertically and laterally heterogeneous and faulted. Although log data from 42 wells are available, the wells are sparsely located. Therefore, in order to adequately characterize the reservoir, a 3-D seismic survey was acquired in 1994. In general, seismic data can be used to estimate reservoir properties using the cross-correlation between acoustic velocity and porosity (e.g. Domenico, 1984).

Doyen (1988) first introduced cokriging to estimate the average porosity distribution in a reservoir. Since then geostatistical techniques which use 3-D seismic data (e.g. cokriging and sequential gaussian cosimulation, Almeida, 1993) have been widely used in the industry to estimate the distribution of reservoir properties. Geostatistical simulation techniques produce equi-probable multi-realizations of reservoir properties. These techniques support reservoir management in evaluating reserves or selecting drilling locations.

However, if the reservoir layer is thinner than seismic resolution, then the well data may not correlate with the seismic data. In this case only average reservoir properties (e.g. porosity, water saturation, net thickness, etc.) can be estimated. Estimated reservoir properties may also be limited by the frequency bandwidth of seismic data, low signal-to-noise ratio, and ambiguous physical relationships with seismic data. Most of the industry's efforts are focused on such cases (Bashore and Araktingi, 1994).

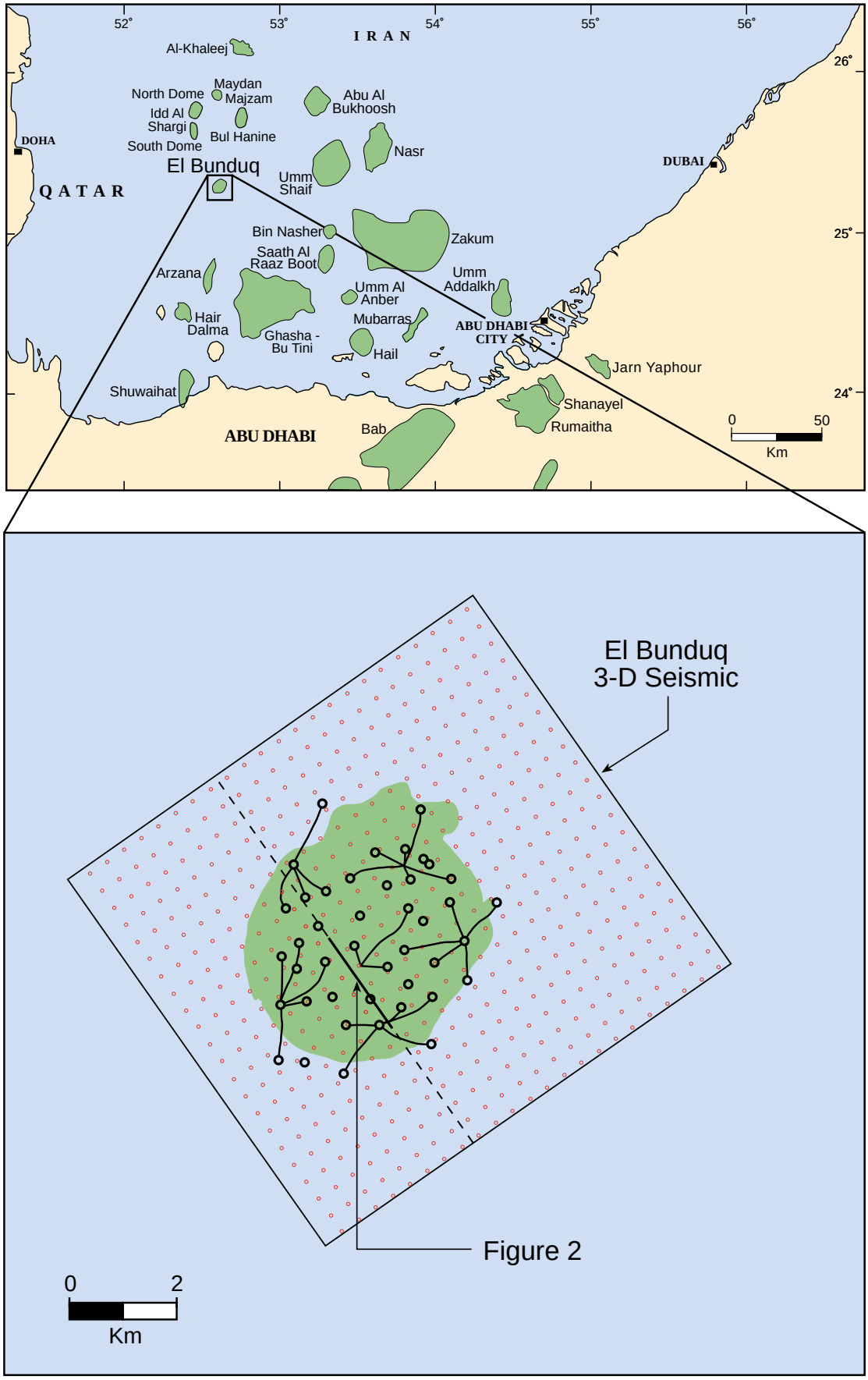

Figure 1: Location of El Bunduq field, wells and 3-D seismic. Thick line indicates the location of the section shown in Figure 2.

In the case of the Arab C4 reservoir in El Bunduq, the seismic wavelets extracted near the wells are unstable and the thickness of the reservoir is less than the seismic resolution. Also the seismic attributes individually have weak cross-correlation coefficients (<0.5) to reservoir properties. In such an extreme case the neural network technique may be effective in relating seismic attributes to reservoir properties.

In this study the reservoir property of interest is porosity-thickness ∑øh. Johnston (1993) used a similar method to predict the areal distribution of sand / shale percentage. We evaluate the application of three methods to predict the spatial distribution of ∑øh for El Bunduq Arab C4 reservoir. The first is simple kriging using only wells. The second is the neural network technique. The third method uses the output of the neural network as soft data for cokriging. In this study we also perform cross-validation tests to examine the reliability of the neural network approach.

DATA ANALYSIS

The primary objectives in this study are the application of neural networks and geostatistics to an actual oil field, and examining its validity.

General processing flow is as follows:

(1) Extract seismic attributes.

(2) Train the neural networks. The reservoir property from well log data and the seismic attributes at well locations are used in the learning data set.

(3) The trained network is applied to the whole processing area.

(4) Cokriging is applied using the result of (3) as soft data, where the data derived from the well logs are used as hard data.

The data set used here is 3-D seismic data and log data of 42 wells. Twenty-seven of these are deviation wells. The reservoir property to be processed is ∑øh. An example of the interpreted seismic record (Final Migrated Stack) is shown in Figure 2. Several straight lines with steep angles represent normal faults, while the lower horizon is interpreted as the top of Arab D. The upper horizon was bulk shifted 20 msec from the lower horizon. From the time window between the upper and the lower, we extracted the six types of amplitude statistics, the four types of complex trace statistics, and the two types of sequence statistics as follows:

Amplitude statistics
- RMS Amplitude
- Average Absolute Amplitude
- Maximum Peak Amplitude
- Average Peak Amplitude
- Maximum Trough Amplitude
- Average Trough Amplitude

Complex trace statistics
- Average Reflection Strength
- Average Instantaneous Frequency
- Slope of Reflection Strength
- Slope of Instantaneous Frequency

Sequence statistics
- Energy Half Time
- Ratio of Positive / Negative

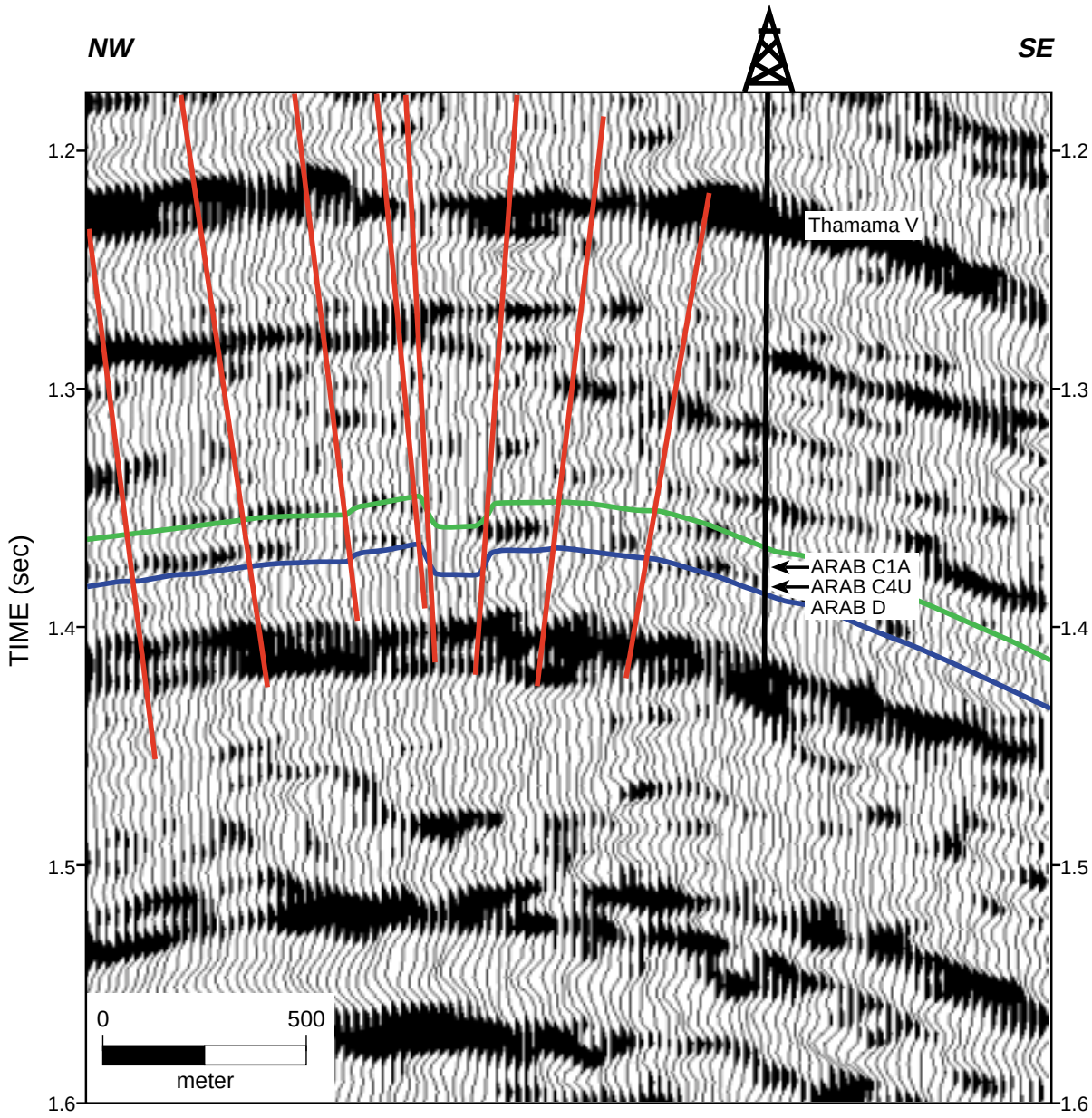

Figure 2: An example of interpreted seismic sections. The steep lines (shown in red) represent normal faults. The lower horizon (shown in blue) corresponds to the top of Arab D, and the upper (shown in green) is the bulk-shifted horizon, 20 msec from the Arab D.

Brown (1987) provides an overview of the value of seismic amplitude. In respect to the complex trace statistics, which were introduced by Taner et al. (1979), White (1991) gives an overview of their physical meaning. Then, from the window of 40 msec above the lower horizon, the following 5 attributes were extracted:

Peak Spectral Frequency
Spectral Slope from Peak to Maximum Frequency
Dominant Frequency Series F1
Dominant Frequency Series F2
Dominant Frequency Series F3

In calculating the above spectral statistics, the maximum entropy method (Burg, 1967) is used to convert the input to the frequency domain within a limited time window.

Although the calibrated time thickness of the Arab C4 are generally less than 20 msec, the window was extended. The reason is that a sufficient number of samples is necessary for the calculation of attributes (sampling rate 4 msec). For the training data set of neural networks, travel time and amplitude extracted from the lower horizon, X-Y coordinates were added to the above attributes.

Figure 3 illustrates the neural networks used to predict ∑øh. The input layer has 21 elements which correspond to each of the seismic attributes. These elements are connected to the hidden layer which consists of 14 elements. In turn each of the elements of the hidden layer is connected to the output ∑øh and Bias, which is also connected to the output. The extracted attributes at 42 well locations are input to train the neural networks. Once training is complete, the network is applied to the whole gridded seismic data. The grid cell size here is 100 by 100 m.

The predicted ∑øh distribution is shown in Figure 4a. Figure 4b shows a cross-plot between the value derived well log data and the estimated value at 42 well locations. This figure clearly indicates that the trained networks reproduce the teacher values with an error less than 1%.

In the next step, cokriging is applied using the grid data estimated by the trained networks as soft data. In this case, when the lag (h) is zero, the cross-correlogram is 1 ($C_{pt}(0)/\sigma_p\sigma_t = 1$). Therefore, if cokriging is applied as it is, the estimation will be almost equivalent to the neural networks output (Figure 4a). Therefore, we neglected the cross-correlogram at h=0 and modeled the spatial connectivity function in the range h≥100 m (see Figure 5). As shown in Figure 5, the cross-correlogram at h=0 has been set to be 0.75. Figure 6a shows the cokriged ∑øh distribution, and Figure 6b is that of the estimated standard deviation. For the comparison, the ∑øh distribution by simple kriging is shown in Figure 6c and its standard deviation in Figure 6d.

White small circles in Figure 6 indicate the well locations across the reservoir unit. The cokriged distribution in Figure 6a is more heterogeneous than the kriged in Figure 6c. The standard deviation in Figure 6b is smaller than the that in Figure 6d.

In the next section, the validity of the above method which is a combination of neural networks and cokriging will be investigated by some cross-validation tests.

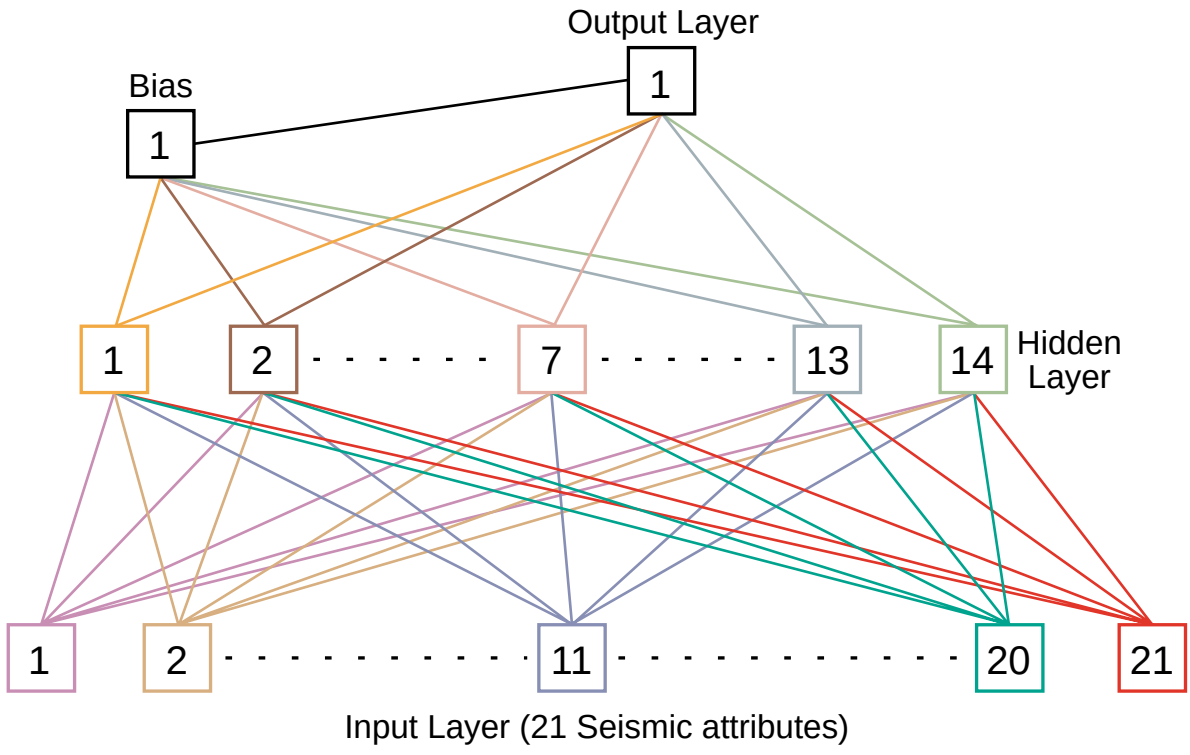

Figure 3: Neural network used in this study.

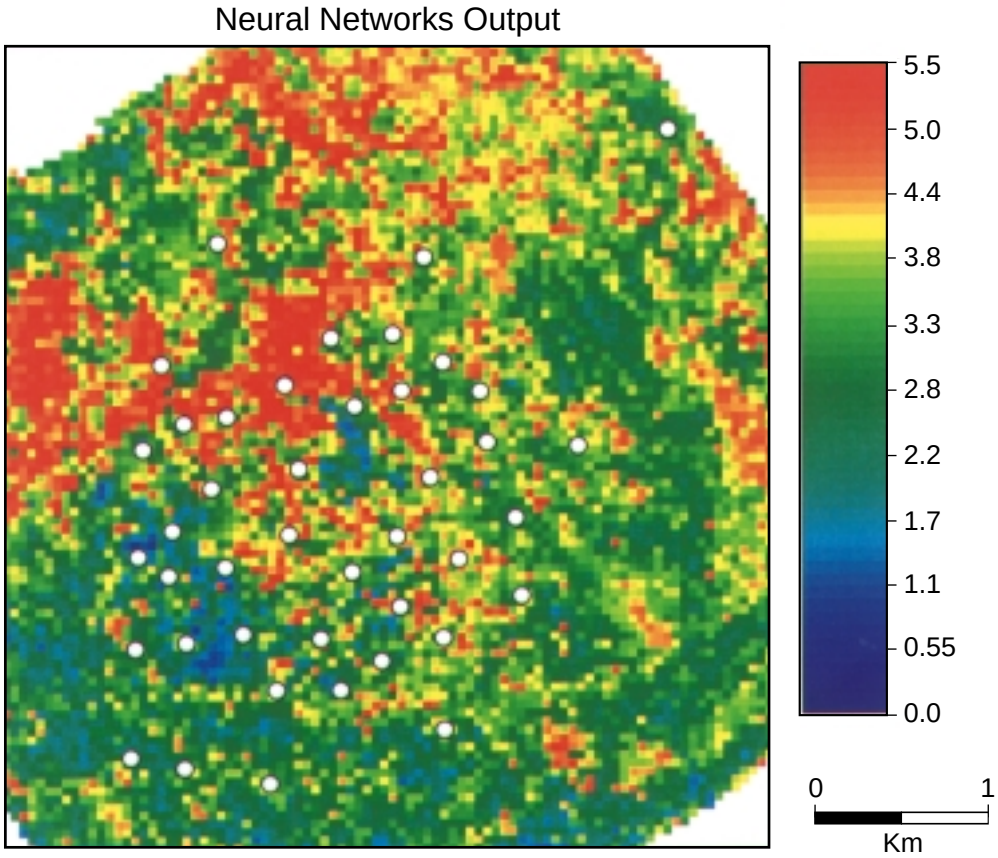

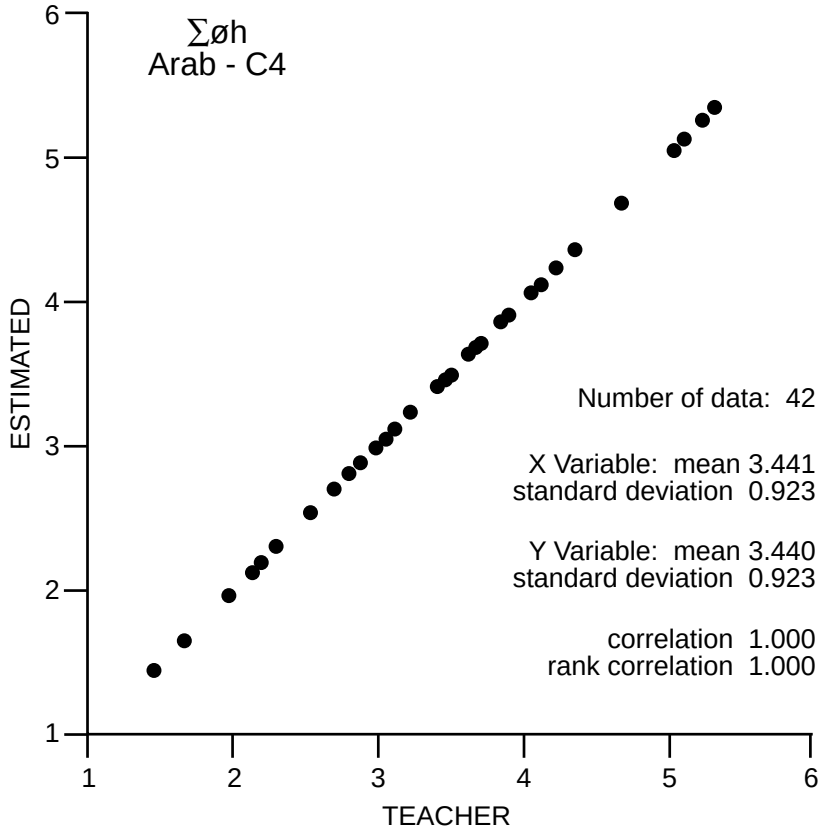

Figure 4: (a) Estimated ∑øh distribution map by the neural network. Small circles show the well locations across the reservoir unit. (b) The cross-plot between neural networks estimations and well data. The trained networks reproduce the teacher values with the error less than 1%.

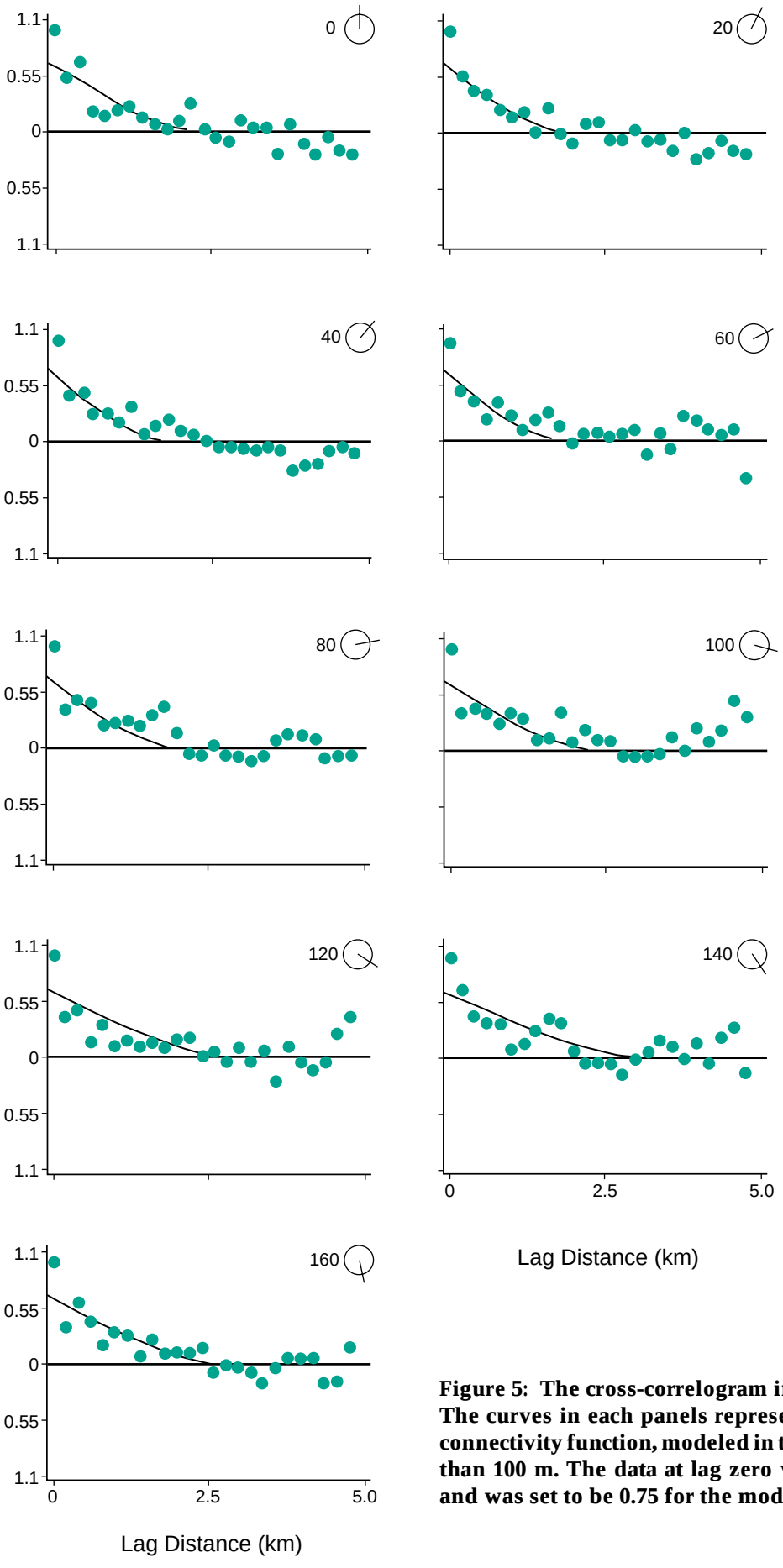

Figure 5: The cross-correlogram in 9 directions. The curves in each panels represent the spatial connectivity function, modeled in the range more than 100 m. The data at lag zero was neglected and was set to be 0.75 for the model function.

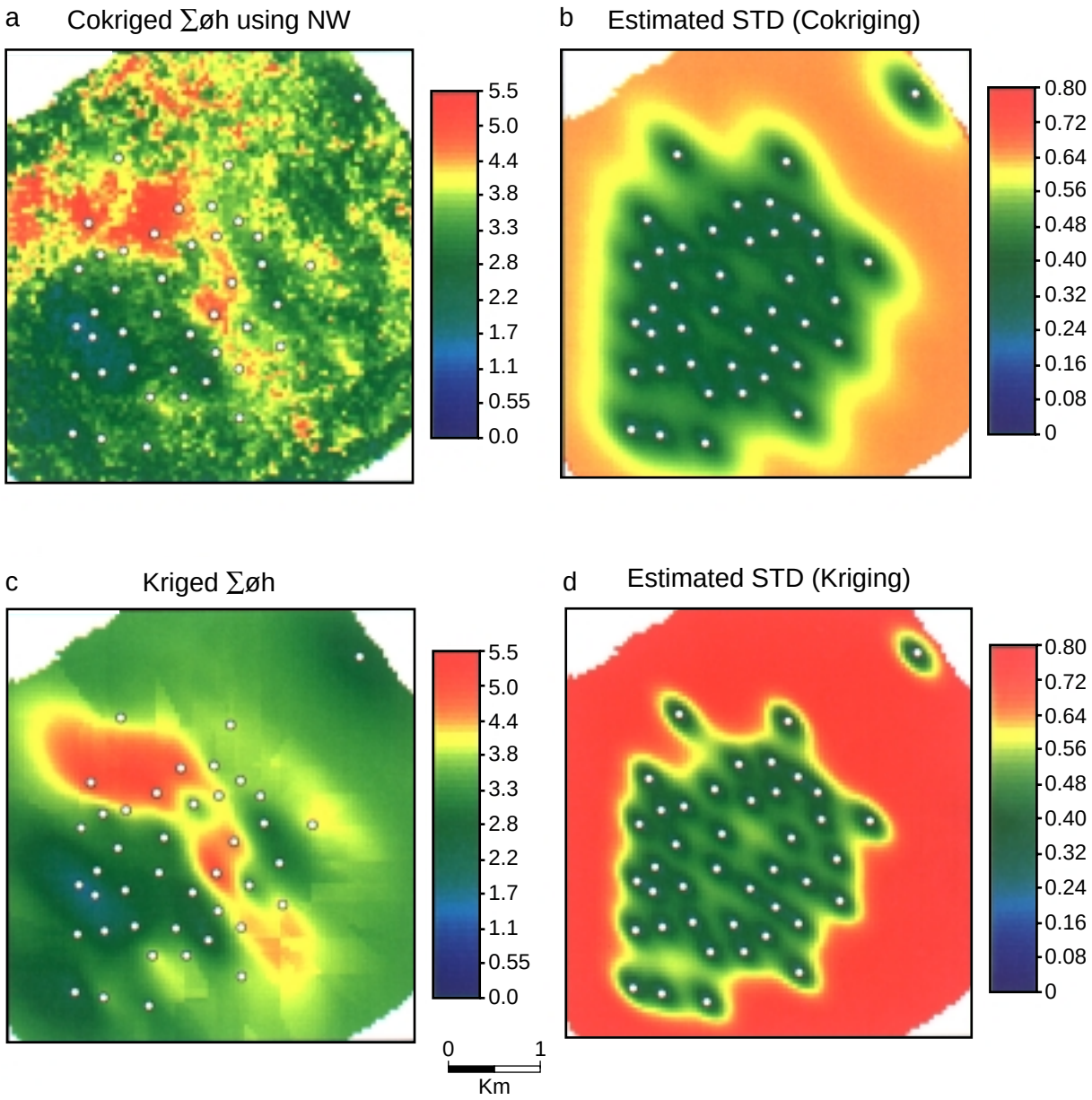

Figure 6: (a) Cokriged ∑øh distribution. (b) The estimated standard deviation by cokriging. (c) Kriged ∑øh distribution. (d) The standard deviation by kriging. White small circles in each figures indicate the well locations across the reservoir unit.

Cross-validation Tests

We use the following two approaches for the cross-validation tests.

Test I. One well is removed from all. The estimated value is checked at the hidden well location.

Test II. Analyze using only 15 vertical wells. Check the estimated value at the 27 hidden wells.

The following three characterization approaches are compared for each of the above two tests.

Method I. Simple Kriging
Method II. Neural Networks
Method III. Neural Networks + Cokriging

Test I

In this cross-validation test, each of the 42 wells in turn was hidden in the analysis by the above 3 methods, and the estimated value was checked at the hidden well location for each method.

Figure 7 shows the example in which the estimations at the hidden well location are close to the actual data. The distribution maps estimated by Methods I, II and III are shown in Figure 7a, 7b and 7c, respectively. The example in which the estimates at the hidden well are much different from the actual data is shown in Figure 8. The layout of distribution maps are the same as shown in Figure 8.

After such tests had been applied for each of the 42 wells, the results of Test I were summarized in Figure 9. The cross-plots between the actual data and the estimation at the hidden well location, for Method I, II, and III, is shown in Figure 9a, b, and c, respectively. The largest dispersion is seen for Method II, neural networks only, as shown in Figure 9b. The dispersion for Method I (Figure 9a) is almost the same as that for Method III (Figure 9c).

For Method I and Method III, the errors between the actual data and the estimation data were compared to the estimated standard deviations. For Method I, the error exceeded the estimated standard deviation,

$$|\sum \text{øh}_{est} - \sum \text{øh}_{obs}| > \sigma_{est}$$

in 23 cases, and for Method III, exceeded in 24 cases. As a result, it seems that neural networks output as soft data does not necessarily contribute to an accurate estimation.

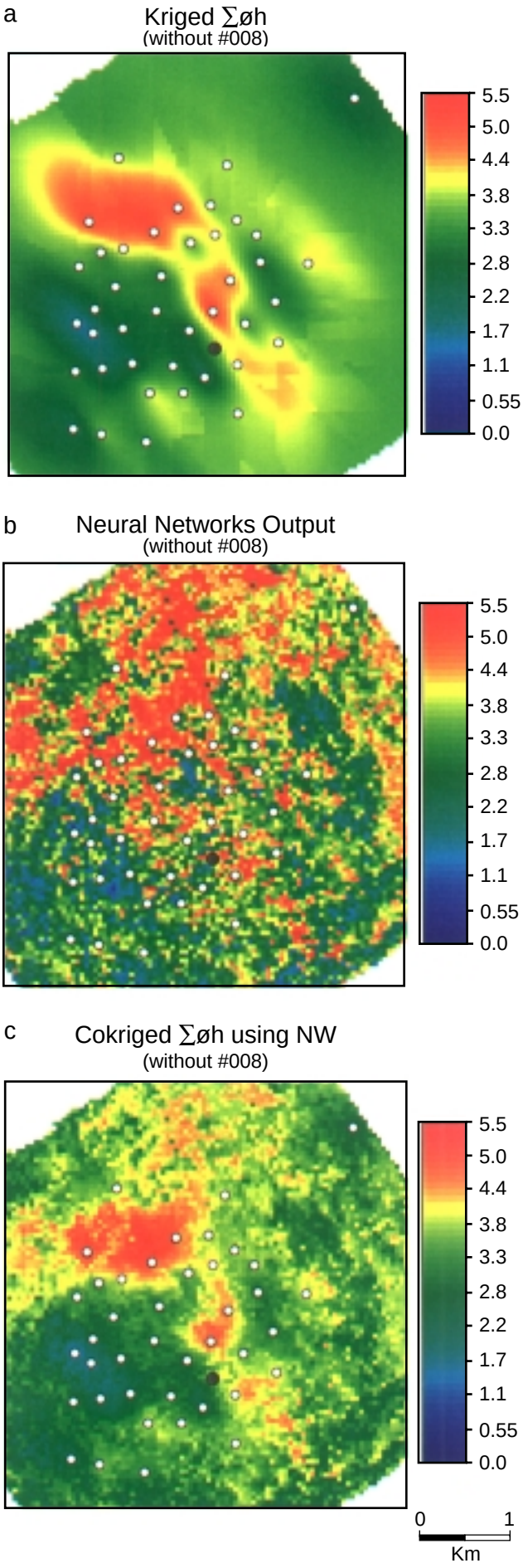

Figure 7: The cross-validation test hiding well #008 (Test I). (a) The ∑øh distribution map by kriging (Method I), (b) by neural networks (Method II), and (c) by cokriging using neural networks output (Method III). White small circles in each figures indicate the well locations across the reservoir unit. The gray larger one shows the hidden well. These estimations are close to the actual data.

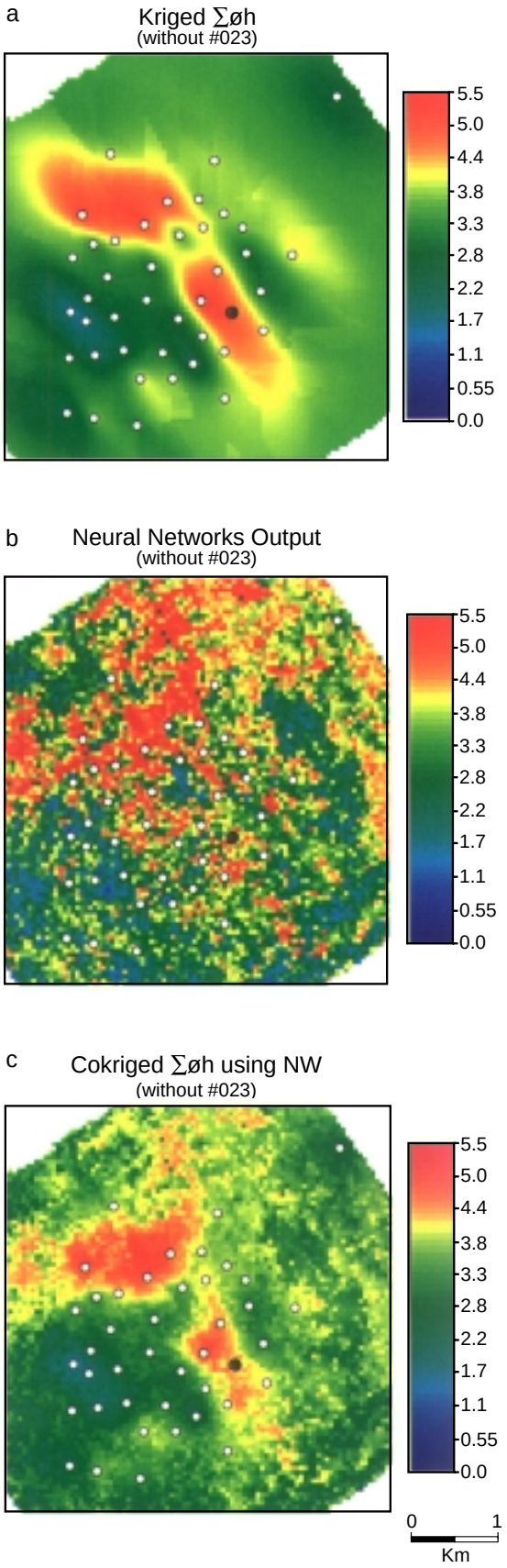

Figure 8: The cross-validation test hiding well #023 (Test I). (a) The ∑øh distribution map by kriging (Method I), (b) by neural networks (Method II), and (c) by cokriging using neural networks output (Method III). The symbols are same as in Figure 7. These estimations are much different from the actual data.

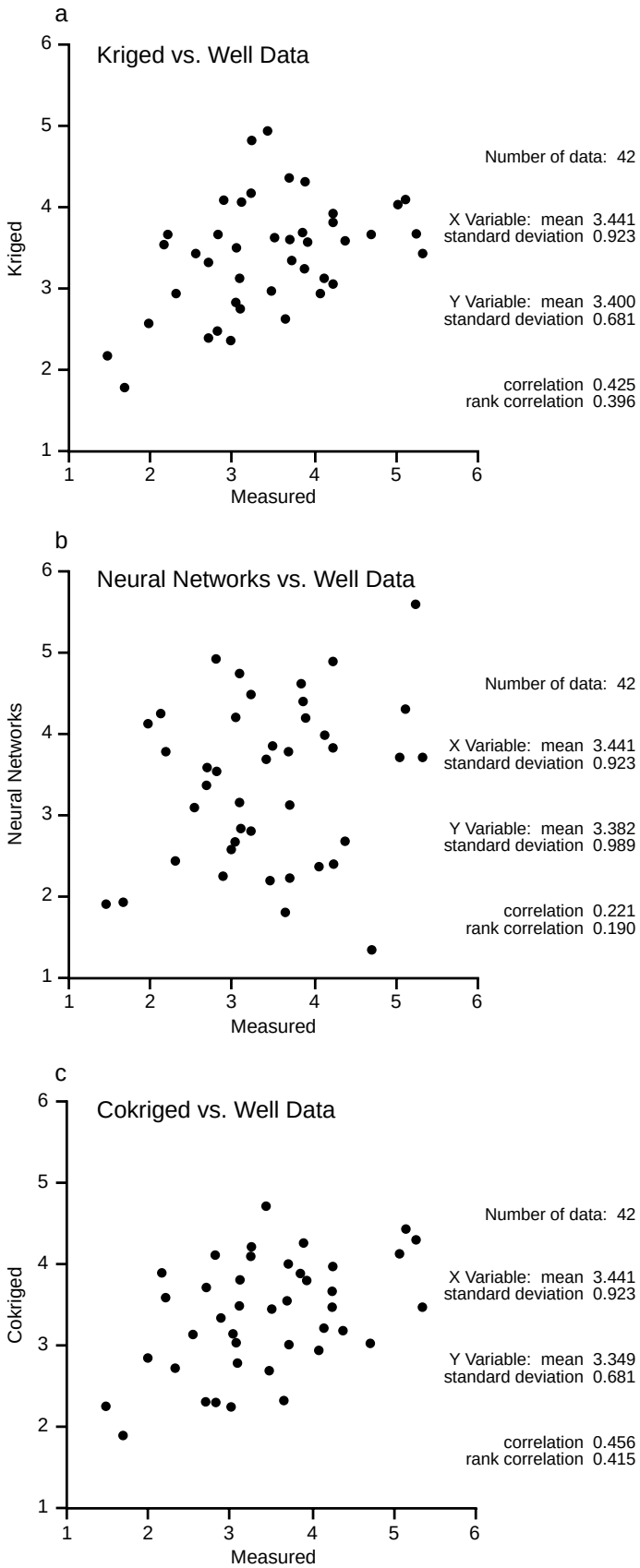

Figure 9: The results of the cross-validation test (Test I) are summarized in cross-plots between the estimation at hidden well locations and the actual data (a) for Method I, (b) for Method II, and (c) for Method III. The largest dispersion is seen in (b). The dispersion of (c) is slightly smaller than that of (a).

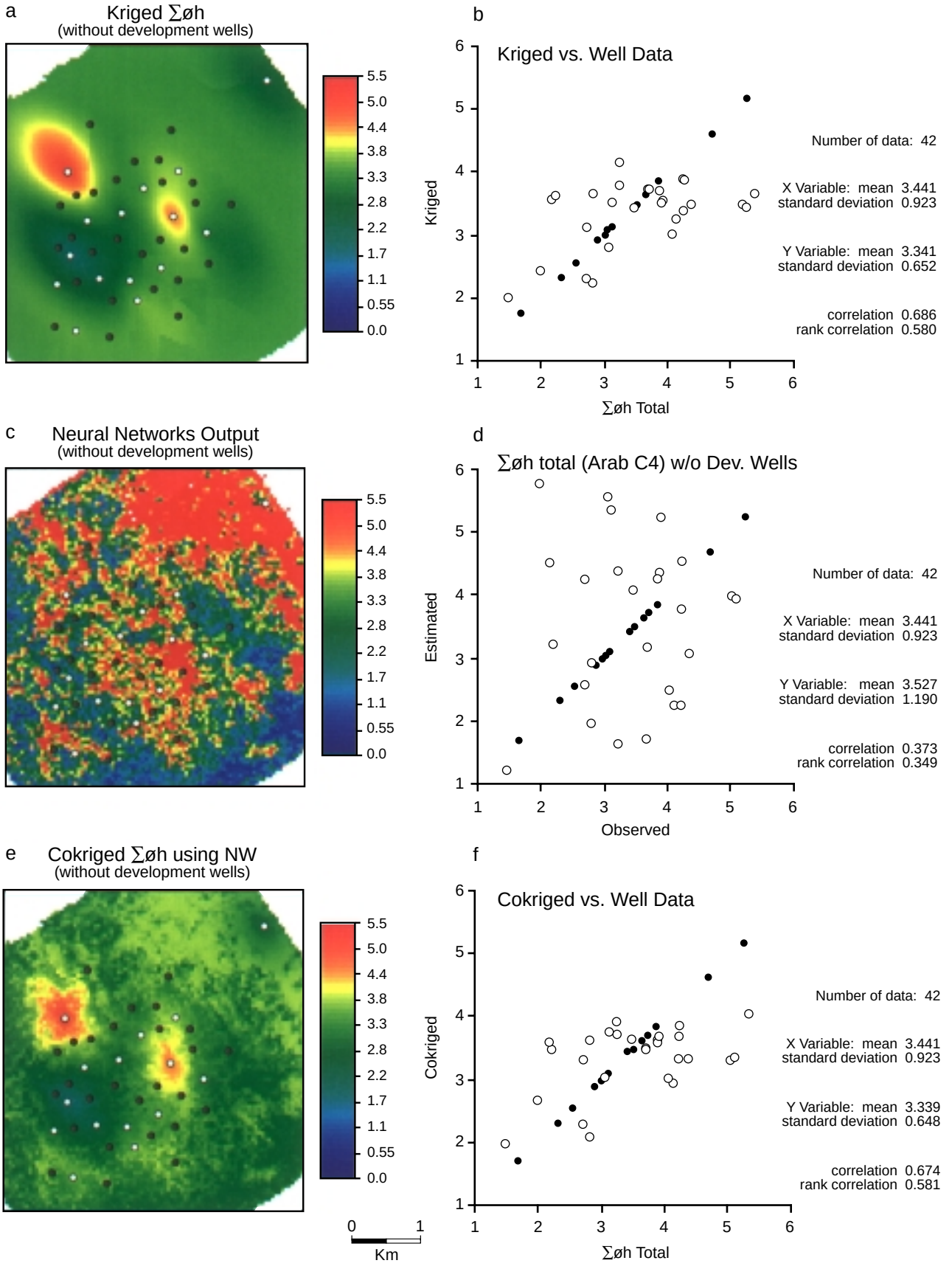

Figure 10: The cross-validation test hiding 27 deviation wells (Test II). (a) The ∑øh distribution map by kriging (Method I) and (b) its cross-plot between the estimations and the actual data, (c) by neural networks (Method II) and (d) its cross-plot, and (e) by cokriging using neural networks output (Method III) and (f) its cross-plot. The gray circles indicate the hidden wells. The largest dispersion is seen in (d). The dispersion of (f) is almost same as that of (b).

Test II

In Test II, the 3 analyses by Method I, II, and III were done, using only 15 wells. Then, the estimated value was checked at 27 hidden well locations for each method. The result is summarized in Figure 10. Figure 10a, Figure 10c, and Figure 10e show the estimated $\sum \phi h$ distributions by Method I, II, and III, respectively. The cross-plots between the actual and the estimated values by Method I, II, and III are shown in Figure 10b, d and f, respectively. The larger gray circles represent the hidden well data in each of the graphs of Figure 10.

As in Test I, the largest dispersion is seen when using Method II (Figure 10d). The dispersion for Method I (Figure 10b) is almost the same as that for Method III (Figure 10f). For Method I, the error exceeded the estimated standard deviation,

$$|\sum \phi h_{est} - \sum \phi h_{obs}| > \sigma_{est}$$

at 11 hidden well locations, while Method III, exceeded it at 15 locations. In Test II, it also seems that the estimation accuracy is not always improved, even if using the neural networks output as soft data for cokriging.

CONCLUSIONS

A case study of reservoir characterization was described. Neural networks and geostatistical approach were applied, using 3-D seismic data acquired in El Bunduq field. Significant correlation cannot be recognized between the reservoir property to be estimated and each of the seismic attributes. One reason is that the wave length of seismic traces, final migrated stack data, seemed to be approximately 7 times longer than the reservoir thickness (10 to 15 m) to be analyzed. Another reason is the poor S/N ratio of seismic data.

In order to overcome this problem, we tried to apply neural networks, inputing the multi-variables. Though each of the seismic attributes had only weak cross-correlation, the output from the trained neural network are consistent with actual well data, which were used as teacher values in a training data set. Then, cokriging was applied using neural networks output as soft data. This approach can provide plausible distribution maps, which honor both well data and the spatial variation of seismic data.

However, by conducting cross-validation tests, it was found that relatively large dispersion between the actual data and the estimation can occur in the case of applying only neural networks (Method II). Consequently, it seems that cokriging using neural networks output (Method III) cannot always estimate precisely, compared with kriging using only well data (Method I). Furthermore, it is possible that the risk of evaluation error at unknown data points becomes larger, because standard deviations estimated in cokriging are less than in kriging. That is, neural networks can easily generate a strong cross-correlation using multi-variables, but they make it difficult to evaluate uncertainties because their physical relationships are left ambiguous.

In the future, improved seismic data is a requisite. Also we need to investigate the sensitivity in changing neural networks structure. For example, limiting the types of seismic attributes to input, or adding and reducing the number of processing elements in the hidden layer. It is also necessary to check the sensitivity in changing the time window over which seismic attributes are extracted.

ACKNOWLEDGMENTS

The authors are grateful to Abu Dhabi National Oil Company, Qatar General Petroleum Corporation, Bunduq Company Limited and United Petroleum Development Company Limited for permission to publish this paper. We also especially thank Mr. Yonebayashi, Reservoir Engineer, JNOC-TRC, for providing us the results of well log analysis, and Ms. Tani, Computer Scientist, FUJI-RIC, for advising on neural networks technique.

REFERENCES

Almeida, A.S. 1993. *Joint Simulation of Multiple Variables with a Markov-type Coregionalization Model.* Stanford Center for Reservoir Forecasting Annual Report.

Bashbush, J.L., W.K. Savage and R.B. Nagai 1983. *A Reservoir Optimization Study - El Bunduq Field.* Abu Dhabi, Qatar. SPE No. 11481, p. 323-333.

Bashore, W.M. and U.G. Araktingi 1994. *Seismic Inversion Methodology for Reservoir Modeling.* Presented at GEO'94 Middle East Geosciences Conference.

Brown, A.R. 1987. *The Value Of Seismic Amplitude.* The Leading Edge, v. 6, no. 10, p. 30-33.

Burg, J.P. 1967. *Maximum Entropy Spectral Analysis.* SEG 37th Annual International Meeting, October, Oklahoma City.

Domenico, S.N. 1984. *Rock Lithology And Porosity Determination from Shear and Compressional Wave Velocity.* Geophysics, v. 49, no. 8, p. 1188-1195.

Doyen, P.M. 1988. *Porosity from Seismic Data: A Geostatistical Approach.* Geophysics, v. 53, no. 10, p. 1263-1275.

Honda, N., Y. Obata and M.K.M. Abouelenein 1989. *Petrology and Diagenetic Effects of Carbonate Rocks: Jurassic Arab C Oil Reservoir in El Bunduq Field, Offshore Abu Dhabi and Qatar.* SPE no. 18006, p. 787-796.

Johnston, D.H. 1993. *Seismic Attribute Calibration Using Neural Networks.* 63rd Annual Meeting of the Society of Exploration Geophysicists, Expanded Abstracts, p. 250-253.

Taner, M.T., F. Koehler and R.E. Sheriff 1979. *Complex Seismic Trace Analysis.* Geophysics, v. 44, p. 1041-1063.

White, R.E. 1991. *Properties of Instantaneous Seismic Attributes.* The Leading Edge, v. 10, no. 7, p. 26-32.

ABOUT THE AUTHORS

Katsuhei Yoshioka *has four years of exploration experience of which one year was with JAPEX Geoscience Institute Ltd. and 3 years with Japan Petroleum Exploration Co. Ltd. He has been working at the Technology Research Center of Japan National Oil Corporation since 1993. Katsuhei has a BSc in Geophysics and a MSc in Seismology from Kyoto University.*

Nobusuke Shimada *received his BSc (1983) and MSc (1985) in Geophysics from Tohoku University, Japan. Since joining Japan National Oil Corporation in 1985, he has been working in project evaluations and geophysical surveys for Japanese and overseas projects. Nobusuke is currently an Assistant Director of Geophysical Laboratory in Technical Research Center of JNOC. His current interests are reservoir geophysics and reservoir characterization.*

Yoshiro Ishii *is currently the Assistant General Manager of JNOC Middle East Representative Office in Bahrain. He received his BSc from Tokai University and joined JNOC in 1981. He had been working for new project evaluation and implementation of geophysical surveys around the world including Oman, Jordan and Myanmar. From 1992 to 1995 Yoshiro was Head of Reservoir Geophysics Group at the Technology Research Center (JNOC/TRC). His current responsibilities are not limited to technologies but include all matters concerning the Middle East.*

Paper presented at the 2nd Middle East Geosciences Conference and Exhibition, GEO'96, Bahrain, 15-17 April 1996

Manuscript Received 15 March 1996

Revised 13 August 1996

Accepted 28 August 1996